Efficient Raman Enhancement and Intermittent Light Emission Observed in Single Gold Nanocrystals

John T. Krug, II, Geoffrey D. Wang, Steven R. Emory, and Shuming Nie*

Contribution from the Department of Chemistry, Indiana University, Bloomington, Indiana 47405

Received June 17, 1999

Abstract: This paper reports two fundamental observations on the size-dependent optical properties of colloidal gold nanoparticles. First, faceted gold nanocrystals in the size range of 63 ± 3 nm have been found to be highly efficient for surface-enhanced Raman scattering (SERS). These nanocrystals are identified from a heterogeneous population for large optical enhancement at 647-nm laser excitation. Second, spatially isolated single gold particles emit Stokes-shifted Raman photons in an intermittent on-and-off fashion. In contrast to population-averaged studies, blinking surface-enhanced Raman scattering is a signature of single-particle (or even single-molecule) behavior. By directly measuring optical enhancement and time-resolved emission on single nanoparticles, this work opens new possibilities in studying the mechanisms of SERS, in developing metal tips for near-field optical microscopy, and in designing new nanostructured materials.

Introduction

Metal and semiconductor particles on the nanometer scale have unique optical, electronic, and magnetic properties that are not available in either isolated molecules or bulk solids.[1] These properties are currently under intense study for potential uses as optoelectronic components,[2] spectroscopic enhancers,[3] biological detection labels,[4] and chemical sensing elements.[5] However, current research is based mainly on population-averaged measurements, in which a large number of nanoparticles are studied and their average responses are recorded. These experiments yield only population-averaged results and not the intrinsic or fundamental properties. This problem has gradually been overcome by ultrasensitive optical imaging and spectroscopy at the level of single molecules and single nanoparticles.[6] These studies can yield new and novel insights that are not available from traditional ensemble-based measurements. For example, discontinuous fluorescence emission has been observed in a number of single quantum systems such as single dye molecules,[7] single fluorescent proteins,[8] single conjugated polymers,[9] and single CdSe quantum dots.[10]

With the use of surface-enhanced Raman scattering (SERS),[11] we have discovered a new class of silver colloidal nanoparticles that is extremely efficient for surface optical enhancement.[12] Independently, Kneipp and co-workers[13] have reported enormous Raman enhancement on aggregated silver particle clusters with near-infrared laser excitation. The observed enhancement factors are on the order of $10^{14}-10^{15}$, much larger than the ensemble-averaged values (10^6-10^8) derived from conventional measurements. Following these initial studies, Käll and co-workers[14] have confirmed the presence of optically "hot" silver particles and have reported single-molecule SERS spectra for nonfluorescent biomolecules such as hemoglobin and tyrosine. Furthermore, Trautman, Brus, and co-workers[15] have obtained

* To whom correspondence should be addressed. E-mail: nie@indiana.edu.

(1) (a) Alivisatos, A. P. *Science* **1996**, *271*, 933−937. (b) Brus, L. E. *Appl. Phys. A* **1991**, *53*, 465−474. (c) Henglein, A. *Chem. Rev.* **1989**, *89*, 186101873. (d) Weller, H. *Angew. Chem., Int. Ed. Engl.* **1993**, *32*, 41−53.

(2) (a) Reed, M. A. *Sci. Am.* **1993** (January), 118−123. (b) Fafard, S.; Hinzer, K.; Raymond, S.; Dion, M.; McCaffrey, J.; Feng, Y.; Carbonneau, S. *Science* **1996**, *274*, 1350−1353.

(3) (a) Lyon, L. A., Musick, M. D., Natan, M. J. *Anal. Chem.* **1998**, *70*, 5177−5183. (b) Keating, C. D., Kovaleski, K. M., Natan, M. J. *J. Phys. Chem. B.* **1998**, *102*, 9404−9413. (c) Van Duyne, R. P.; Hulteen, J. C.; Treichel, D. A. *J. Chem. Phys.* **1993**, *99*, 2101−2115.

(4) (a) Chan, W. C. W.; Nie, S. *Science* **1998**, *281*, 2016−2018. (b) Bruchez, M., Jr.; Moronne, M.; Gin, P.; Weiss, S.; Alivisatos, A. P. *Science* **1998**, *281*, 2013−2018.

(5) (a) Storhoff, J. J.; Elghanian, R.; Mucic, R. C.; Mirkin, C. A.; Letsinger, R. L. *J. Am. Chem. Soc.* **1998**, *120*, 1959−1964. (b) Elghanian, R.; Storhoff, J. J.; Mucic, R. C.; Letsinger, R. L.; Mirkin, C. A. *Science* **1997**, *277*, 1078−1081. (c) Weissman, J. M.; Sunkara, H. B.; Tse, A. S.; Asher, S. A. *Science* **1996**, *274*, 959−960. (d) Holtz, J. H.; Asher, S. A. *Nature* **1997**, *389*, 829−832.

(6) For reviews, see: (a) Moerner, W. E.; Orrit, M. *Science* **1999**, *83*, 1670−1676. (b) Xie, X. S.; Trautman, J. K. *Annu. Rev. Phys. Chem.* **1998**, *59*, 441−480. (c) Nie, S.; Zare, R. N. *Annu. Rev. Biophys. Biomol. Struct.* **1997**, *26*, 567−596. (d) Keller, R. A.; Ambrose, W. P.; Goodwin, P. M.; Jett, J. H.; Martin, J. C.; Wu, M. *Appl. Spectrosc.* **1996**, *50*, 12A-32A.

(7) (a) Trautman, J. K.; Macklin, J. J.; Brus, L. E.; Betzig, E. *Nature* **1994**, *369*, 40−42. (b) Ambrose, W. P.; Goodwin, P. M.; Martin, J. C.; Keller, R. A. *Science* **1994**, *265*, 364−367. (c) Lu, H. P.; Xie, X. S. *Nature (London)* **1997**, *385*, 143−146.

(8) Dickson, R. M.; Cubitt, A. B.; Tsien, R. Y.; Moerner, W. E. *Nature (London)* **1997**, *388*, 355−358.

(9) (a) Vanden Bout, D. A.; Yip, W.-T.; Hu, D.; Fu, D.-K.; Swager, T. M.; Barbara, P. F. *Science* **1997**, *277*, 1074−1077. (b) Yip, W.-T.; Hu, D.; Yu, J.; Vanden Bout, D. A.; Barbara, P. F. *J. Phys. Chem. A* **1998**, *102*, 7564−7575.

(10) (a) Nirmal, M.; Dabbousi, B. O.; Bawendi, M. G.; Macklin, J. J.; Trautman, J. K.; Harris, T. D.; Brus, L. E. *Nature* **1996**, *383*, 802−804. (b) S. A. Empedocles, S. A.; Bawendi, M. G. *Science* **1997**, *278*, 2114. (c) Blanton, S. A.; Hines, M. A.; Guyot-Sionnest, P. *Appl. Phys. Lett.* **1996**, *69*, 3905−3907.

(11) (a) Van Duyne, R. P. In *Chemical and Biochemical Applications of Laser;* Moore, C. B., Ed.; Academic Press: New York, 1979; Vol. 4, pp 101−185. (b) Moskovits, M. *Rev. Mod. Phys.* **1985**, *47*, 783−826.

(12) (a) Nie, S.; Emory, S. R. *Science* **1997**, *275*, 1102−1106.

(13) (a) Kneipp, K.; Wang, Y.; Kneipp, H.; Perelman, L. T.; Itzkan, I.; Dasari, R. R.; Feld, M. S. *Phys. Rev. Lett.* **1997**, *78*, 1667−1670. (b) Kneipp, K.; Wang, Y.; Kneipp, H.; Itzkan, I.; Dasari, R. R.; Feld, M. S. *Phys. Rev. Lett.* **1996**, *76*, 2444−2447.

(14) Xu, H.; Bjerneld, E. J.; Kall, M.; Borjesson, L. *The 4th International Workshop on Single Molecule Detection and Ultrasensitive Analysis in the Life Sciences*; Berlin, Germany, September 30 to October 2, 1998.

(15) Trautman, J. K.; Brus, L. E.; *The Nobel Conference on Single Molecule Spectroscopy in Physics, Chemistry, and Biology*; Stockholm, Sweden, June 5−9, 1999.

10.1021/ja992058n CCC: $18.00
Published on Web 09/15/1999

surface-enhanced Raman and resonant Rayleigh scattering spectra on large single silver (Ag) nanocrystals.

In this paper, we report the use of single-particle imaging and spectroscopy to screen a heterogeneous population of gold colloidal nanoparticles for unusual optical properties. We show that faceted gold nanocrystals in a narrow size range are extremely efficient for surface Raman enhancement. We also show that the SERS-active gold nanoparticles exhibit an intermittent light emission behavior on the millisecond-to-second time scales, similar to that observed in single Ag nanoparticles.[16] A surprising finding is that the SERS-active gold particles have a size range of 63 ± 3 nm, much smaller than the active silver particles (190−200 nm) at 647-nm excitation.[17] These sizes refer to diameters for spheres and major/minor axes for ellipsoids.

A significant advantage of studying gold nanoparticles is that relatively monodispersed colloids can be prepared by using simple synthetic procedures.[18−20] Gold colloids are also more compatible with biological molecules, a feature that will be important in developing metal nanoparticles as sensitive biological labels.[3,5] By extending single-particle Raman scattering to gold nanostructures, this work opens new opportunities in studying the fundamental mechanisms of SERS. By correlating particle size and optical enhancement, it might become possible to rationally design efficient and reproducible substrates for surface-enhanced spectroscopy. Single-gold nanoparticles could also be used to expand the current capabilities of near-field scanning optical microscopy (NSOM). As first suggested by Wessel,[21] an optically excited nanoparticle is a highly localized near-field probe because it receives an incident electromagnetic field and amplifies the field by many orders of magnitude. Recently, Xie and co-workers[22] have used metal tips for surface-enhanced near-field optical microscopy and have achieved a spatial resolution of 20 nm.

Experimental Section

Colloid Synthesis and Screening. Gold colloids with various particle sizes were prepared by the citrate-reduction procedure, as originally reported by Frens[18] and modified by Natan and co-workers.[20] The particle size was controlled by the molar ratio of the reducing agent (sodium citrate) and the gold precursor ($KAuCl_4$). Thus, a set of four gold colloids in the size range 25−100 nm was prepared. Direct morphological examination by transmission electron microscopy (TEM) showed that the average particle sizes were 23 ± 5 (standard deviation), 39 ± 7, 74 ± 14, and 100 ± 20 nm, respectively. The gold colloids were more monodispersed than silver, but there were still considerable variations in particle size and shape. For example, statistical analysis showed that the 74-nm colloid had a size variation of 15−20%. High-resolution TEM studies further revealed that these colloidal particles were faceted nanocrystals, with well-developed crystal planes and edges.

For optical screening, freshly prepared gold colloids were stabilized in 0.01% (weight) sodium citrate. Aliquots of the colloids were incubated with a probe molecule (e.g., crystal violet, bipyridine, or mercaptopyridine) for 30 min at room temperature. The particles were immobilized on polylysine-coated glass surfaces by electrostatic interactions between the negative charges on the particles and the positive charges on the surface. An epi-illuminated Raman microscope was used to screen the immobilized particles for SERS activity. With an automated scanning stage, we were able to screen about 5−20 million particles on a standard microscope slide. The SERS-active nanoparticles were observed as bright spots by using a video-rate intensified CCD camera (8-bit or 256 dynamic range) (Photon Technology International, South Brunswick, NJ).

Correlated Optical and AFM Imaging. The identified particles were characterized by using an integrated optical and atomic force microscope. In this instrument, a tapping-mode AFM scanning head (Digital Instruments, Santa Barbara, CA) was mounted directly on an inverted microscope stage. The AFM tip was positioned to a single-particle for nanometer-scale topography, and a laser beam was focused to the same particle for optical spectroscopy. The particle sizes were determined by height measurement because tip convolution makes AFM less accurate in the lateral dimensions.[23] It should be mentioned that this height measurement may not truly reflect the particle size if the particle does not have a regular shape. A more accurate determination might be made by high-resolution TEM, but we were unable to locate specific nanoparticles for correlated optical and TEM measurements.

Confocal Raman Spectroscopy and Time-Resolved Studies. Single-particle Raman spectra were obtained by using a confocal Raman microscope. This instrument consisted of an inverted optical microscope, a single-stage spectrograph (model 270M, Spex, Edison, NJ), and a thermoelectrically cooled CCD detector (Princeton Instruments, Trenton, NJ). Continuous-wave laser excitation at 647 nm was provided by a krypton ion laser (Lexel Laser, Fremont, CA). A long-pass optical filter (Chroma Tech, Brattleboro, VT) was used to reject the scattered laser light and to pass the Raman signals above $\sim$500 cm^{-1}. Time-resolved photon emission data were acquired by using a photon-counting avalanche photodiode (APD) (SPCM-200, EG&G, Vaudreuil, Canada) and a multichannel scalar (EG&G ORTEC, Oak Ridge, TN). A similar apparatus has been used in real-time fluorescence detection of single molecules in solution.[24]

Results and Discussion

Single-Particle Screening and Spectroscopy. Figure 1 shows micro-Raman images obtained from colloidal gold nanoparticles immobilized on polylysine-coated glass surfaces. Tapping-mode AFM measurement reveals that the immobilized colloids are primarily single particles and not aggregates. An important finding is that most of the SERS-active gold particles are present in the 74-nm colloid and that no hot particles are found in the 23- or the 39-nm colloid. For the 100-nm colloid, a small number of particles are weakly active, but this activity could arise from particles that are considerably smaller than the mean particle size. By using a confocal Raman system, we have obtained wavelength-resolved Raman spectra from single gold nanoparticles identified by wide-field screening. Figure 2 shows a single-particle SERS spectrum of crystal violet. The intense signals at 1172, 1217, 1294, 1366, 1389, and 1617 cm^{-1} correspond to Raman-active vibrational modes of crystal violet adsorbed on the particle surface.[13]

To determine the percentage of particles that are SERS-active, we have examined a large number of spatially isolated single particles with an integrated optical and atomic force microscope. In this study, all the immobilized particles were detected by AFM, but only those emitting Stokes-shifted Raman signals were observed in the optical image. The result indicates that only one percent of the gold particles in the 74-nm colloid is highly efficient for enhancement. Surprisingly, quantitative AFM

(16) Emory, S. R.; Nie, S., unpublished results.
(17) Emory, S. R.; Haskins, W. E.; Nie, S. *J. Am. Chem. Soc*. **1998**, *120*, 8009−8010.
(18) Frens, G. *Nature Phys. Sci*. **1973**, *241*, 20−22.
(19) *Colloidal Gold: Principles, Methods, and Applications*; Hayat, M. A., Ed.; Academic Press: New York, 1990; Vol. 1−2.
(20) (a) Freeman, R. G.; Grabar, K. C.; Allison, K. J.; Bright, R. M.; Davis, J. A.; Guthrie, A. P.; Hommer, M. B.; Jackson, M. A.; Smith, P. C.; Walter, D. G.; Natan, M. J. *Science* **1995**, *267*, 1629−1632. (b) Grabar, K. C.; Freeman, R. G.; Hommer, M. B.; Natan, M. J. *Anal. Chem*. **1995**, *67*, 735−743.
(21) Wessel, J. *J. Opt. Soc. Am. B* **1985**, *2*, 1538−1541.
(22) Sanchez, E. J.; Novotny, L.; Xie, X. S. *Phys. Rev. Lett*. **1999**, *82*, 4014−4017.
(23) (a) Ramirez-Aguilar, K. A.; Rowlen, K. L. *Langmuir* **1998**, *14*, 2562−2566. (b) Garcia, V. J.; Martinez, L.; Briceno-Valero, J. M.; Schilling, C. H. *Probe Microsc*. **1997**, *1*, 107−116.
(24) (a) Nie, S.; Chiu, D. T.; Zare, R. N. *Science* **1994**, *266*, 1018−1021. (b) Nie, S.; Chiu, D. T.; Zare, R. N. *Anal. Chem*. **1995**, *67*, 2849−2857.

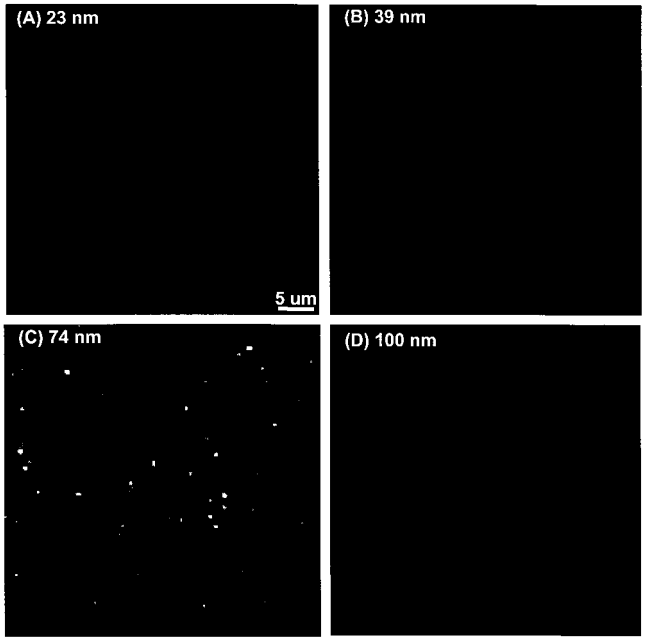

Figure 1. Rapid screening of spatially isolated single colloidal Au nanoparticles for efficient optical enhancement. Raman images were obtained from a set of four colloids that were incubated with 2×10^{-9} M crystal violet in 0.01% sodium citrate water solution. Individual SERS-active nanoparticles were observed as bright spots. The average particle sizes and their standard deviations (s) are: (A) 23 nm ($s = 5$ nm), (B) 39 nm ($s = 7$ nm), (C) 74 nm ($s = 14$ nm), and (D) 100 nm ($s = 20$ nm). Excitation wavelength = 647.1 nm; total wide-field laser power = 20 mW; and integration time = 5 s.

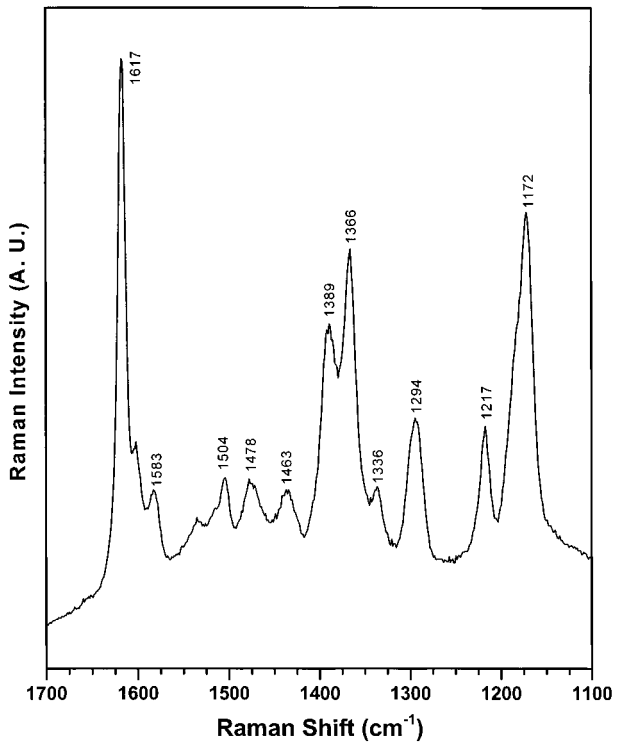

Figure 2. Surface-enhanced Raman scattering spectrum of a single Au nanoparticle with adsorbed crystal violet molecules. Laser wavelength = 647.1 nm; confocal excitation power = 0.1 μW; data integration time = 30 s; and crystal violet concentration = 2×10^{-9} M.

measurement reveals that the most enhancing particles are about 63 nm in diameter, much smaller than the mean particle size (Figure 3). Statistical analysis further shows that the SERS-active particles have a narrow size range, about 63 ± 3 nm. Outside this size range, the particles have little or no SERS activity.

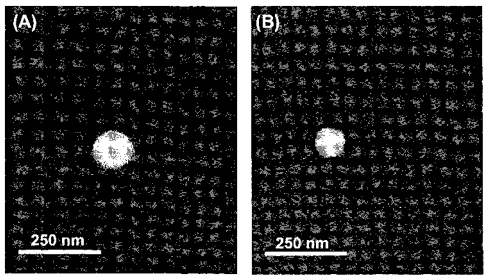

Figure 3. Detailed AFM images of (A) a SERS-**inactive** Au particle (~70 nm diameter) and (B) a SERS-**active** particle (~63 nm diameter). These particles were first examined by wide-field optical imaging at 647-nm laser excitation.

In addition to particle size, there are other factors such as particle shape and specific adsorption sites that are important for efficient optical enhancement.[25] Assuming normal distribution statistics, the number of colloidal particles in the 63 ± 3 nm size fraction would represent ~12% of the total colloid particles (mean particle size 74 nm, standard deviation 14 nm). This value is still higher than the percentage of SERS-active particles, indicating that the majority of particles in this fraction are not efficient for enhancement. This simple analysis suggests that more SERS-active particles could be obtained when the mean particle size approaches the optimal value of 63 nm. To test this hypothesis, we prepared a 60-nm gold colloid by carefully controlling the ratio of the gold precursor and the reducing agent. Figure 4 shows the correlated Raman and AFM images. Indeed, about 10−15% of the particles in this preparation are SERS-active, substantially higher than that in the 74-nm colloid.

These results demonstrate that single particles with novel optical properties can be identified and selected from a heterogeneous population. However, the small size of the optically active gold particles is surprising because the SERS-active Ag particles are as large as 200 nm at the same excitation wavelength.[17] On the basis of the electromagnetic field theory developed by Schatz and co-workers,[26] Ag and gold (Au) nanoparticles in the size range of 150−200 nm are expected to be most efficient for surface Raman enhancement when the excitation wavelength is ~650 nm. This is in good agreement with the measured Ag particle size (190−200 nm), but deviates substantially from the experimental Au particle size (63 nm). Further studies are needed to resolve this discrepancy between experiment and theory.

The narrow size range is also surprising because electromagnetic field calculations would predict a much broader size effect on enhancement.[27] It is possible that the Raman enhancement properties of faceted nanocrystals are different than those of regular ellipsoidal particles (which are used in theoretical modeling). It is also possible that that our experimental data are artificially sharpened by the particle screening and selection

(25) The faceted particle shape could be important for efficient enhancement because the sharp points and edges can act as a "lightning rod" to concentrate the incident electromagnetic field. Also, sharp points, atomic clusters, and adatoms may function as active sites on the particle surface. These special sites are believed to be responsible for chemical Raman enhancement via a resonant charge-transfer process. In comparison with particle size, particle shape and active sites are two factors that are still not well understood.

(26) Zeman, E. J.; Schatz, G. C. *J. Phys. Chem.* **1987**, *91*, 634−643.
(27) Jensen, T. R.; Schatz, G. C.; Van Duyne, R. P. *J. Phys. Chem. B* **1999**, *103*, 2394−2401.

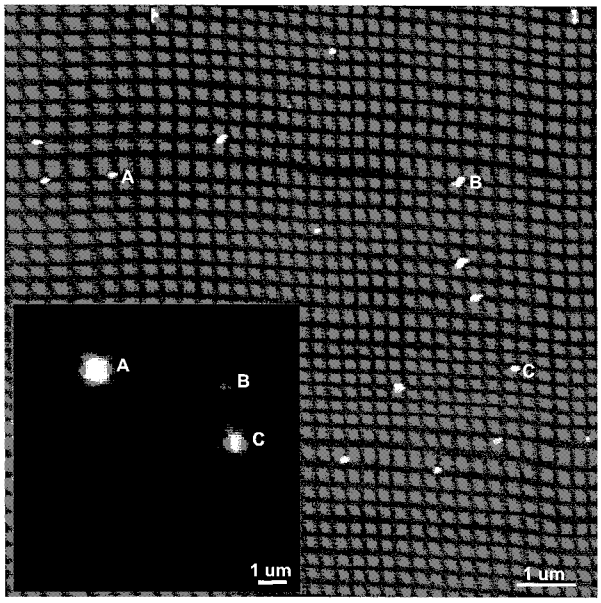

Figure 4. Correlated AFM and surface-enhanced Raman (inset) images of rationally designed colloidal Au nanoparticles (mean particle size = 60 nm). Three SERS-active particles are labeled (A), (B), and (C). Note that particle (B) is an aggregate but its signal intensity is lower than that of particle (A) or (C). Excitation wavelength = 647.1 nm; laser power = 20 mW; and image integration time = 10 s.

process. That is, the most active (intense SERS) particles are preferentially selected for correlated optical and AFM measurements, while the less active particles are not adequately represented in the data set. Recent work by Brus and coworkers[15] indicates that efficient Raman enhancement is not directly correlated with surface plasmon absorption. This raises the possibility that other size-dependent processes might be present, such as size-dependent charge-transfer enhancement.

A common practice in previous SERS studies has been to activate the colloids by electrolyte-induced aggregation.[28] The activated colloid contains large clusters of particles, which are believed to be most efficient for Raman enhancement. To investigate the effect of colloid aggregation on optically hot particles, we prepared Au aggregates by adding 50-mM NaCl to each of the 23-, 39-, 60-, 74-, and 100-nm colloids. The result shows that the SERS intensities are highest for the 60-nm colloid and decrease rapidly for both the 39- and the 100-nm colloids. The nanoaggregates found in the 23-nm colloid yield only weak SERS signals. These results indicate that colloidal aggregation does increase the SERS intensities but does not produce optically "hot" aggregates if the original particles are not active. It should be mentioned that previous SERS studies have mainly used 12−15 nm colloidal Au particles.[20,28] The reported enhancement factors are relatively low (10^4-10^5), even with extensively aggregated colloids or nanoparticle thin films. On the basis of the results of this work, these particles are apparently too small for efficient enhancement. With colloidal Au particles in the size range of 60−70 nm, intense SERS spectra can be obtained with a laser excitation power as low as 60 nW (data not shown). This laser power is about *one million* times lower than those typically used in SERS studies.

Single-Molecule Sensitivity. A number of optical methods based on laser-induced fluorescence have been developed to detect single molecules.[6] They differ in sampling conditions and means of delivering excitation energy, but all of them share the need to isolate single molecules for detection. One approach is to isolate individual molecules spectroscopically in low-temperature solids because matrix perturbations cause each molecule to have a slightly different absorption frequency. A more broadly useful approach is to isolate molecules on a surface or in a dilute solution; that is, individual molecules are spatially separated from each other in the area or volume probed by a laser beam.

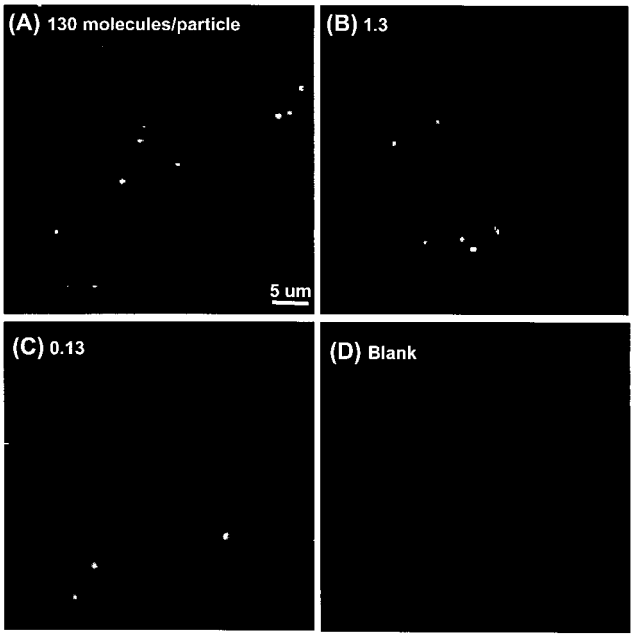

Figure 5. Single-particle Raman images observed at various molecule-to-particle ratios. The same protocol was followed as in Figure 1, except that the analyte concentration (crystal violet) was reduced by serial dilution in water. From (A) to (D), the molecule-to-particle ratio was calculated by dividing the total number of colloidal particles by the total number of added analyte molecules. Excitation wavelength = 647.1 nm; laser power = 50 mW; and image integration time = 10 s.

In this work, the concentration of crystal violet was diluted repeatedly so that the number of analyte molecules is <1 per colloidal particle. Under this condition, the observed signals are believed to arise from single molecules adsorbed at specific surface sites. Figure 5 shows the optical screening results obtained at various molecule-to-particle ratios. In the absence of crystal violet (blank), no SERS signals could be detected. When the number of molecules is much larger than the particles, many particles are observed as bright spots. At a molecule-to-particle ratio of 0.13, only a small number of SERS-active particles are observed by wide-field screening. Quantitative measurement indicates that the SERS signals are weak but constant, similar to those detected at 1.3 molecule-to-particle ratio (Figure 6). Thus, the SERS signals are most likely due to single crystal violet molecules adsorbed on the particle surface. As in the case of silver colloids,[12] the number of detected molecules is smaller than the total number of added analyte molecules. This sublinear relationship can be explained by the fact that crystal violet can adsorb on inactive particles (or at inactive sites) and that some of the analyte molecules remain in free solution (adsorption equilibrium). For rhodamine 6G, it has been estimated that 80% of the dye is adsorbed on the colloidal particles and the remaining 20% stays in solution.[29]

Strictly speaking, the concentration and statistical results alone do not provide conclusive evidence for single-molecule SERS.

(28) *Fundamentals and Applications of Surface Raman Spectroscopy;* Garrell, R. L., Pemberton, J. E., Eds.; VCH Publishers: Deerfield Beach, FL, 1994.

(29) Hildebrandt, P.; Stockburger, M. *J. Phys. Chem.* **1984**, *88*, 5935.

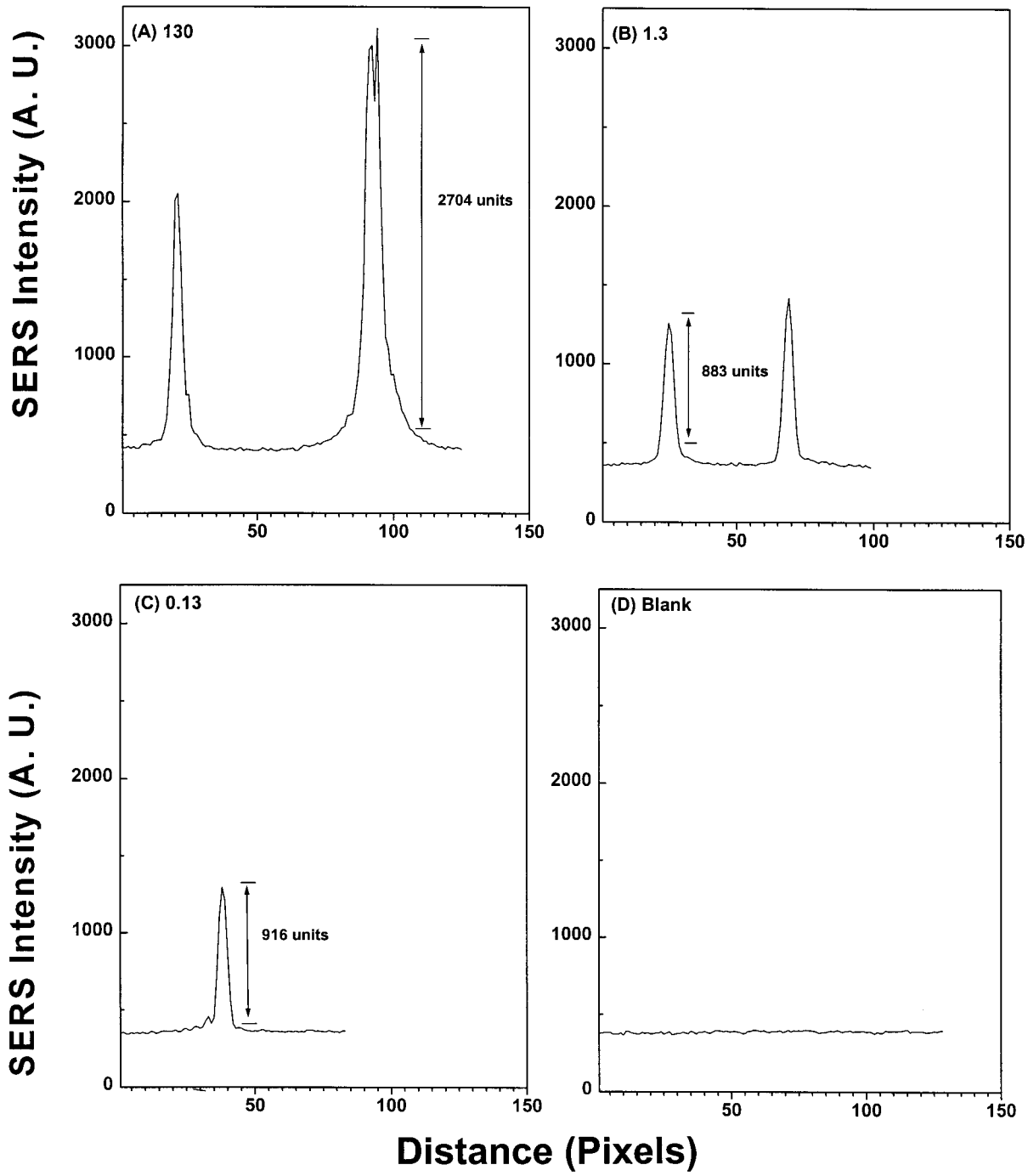

Figure 6. Quantitative measurement of single-particle SERS intensities at ultra-low analyte concentrations. Line plots (A) to (D) correspond to the images in Figure 5.

Other common criteria such as emission polarization, spectral fluctuation, and photochemical bleaching must be carefully examined.[6] We have carried out a comprehensive study on single Ag particles, and the results strongly indicate that single-molecule SERS has been achieved, at least under resonant excitation conditions.[12] On single Au particles, we have only studied the blinking behavior of SERS signals, as discussed in details below. At the lowest molecule-to-particle ratio (0.13−1), it is reasonable to conclude that the observed SERS signals arise from a single or a few molecules adsorbed on the particle surface.

By using the normal Raman scattering signals of methanol as an internal standard,[13] we estimate that the intrinsic enhancement factors on Au are on the order of $10^{13}-10^{14}$. The enhancement factors are calculated by dividing the SERS cross sections of crystal violet by the normal Raman cross sections of methanol (which are similar to those of crystal violet within an order of magnitude). The normal Raman cross sections of crystal violet are difficult to measure because crystal violet has a broad absorption band in the visible region (resonance Raman scattering). Thus, our estimated values represent the total enhancement factors of surface enhancement and resonance enhancement. For nonresonant molecules such as bispyridyl ethylene and mercaptopyridine, the SERS signals are weak when the molecule-to-particle ratio is <1. On the other hand, Kneipp et al.[30] have detected intense SERS signals from nonresonant

(30) Kneipp, K.; Kneipp, H.; Manoharan, R.; Hanlon, E. B.; Itzkan, I., Dasari, R. R., Feld, M. S. *Appl. Spectrosc.* **1999**, *52*, 1493−1497.

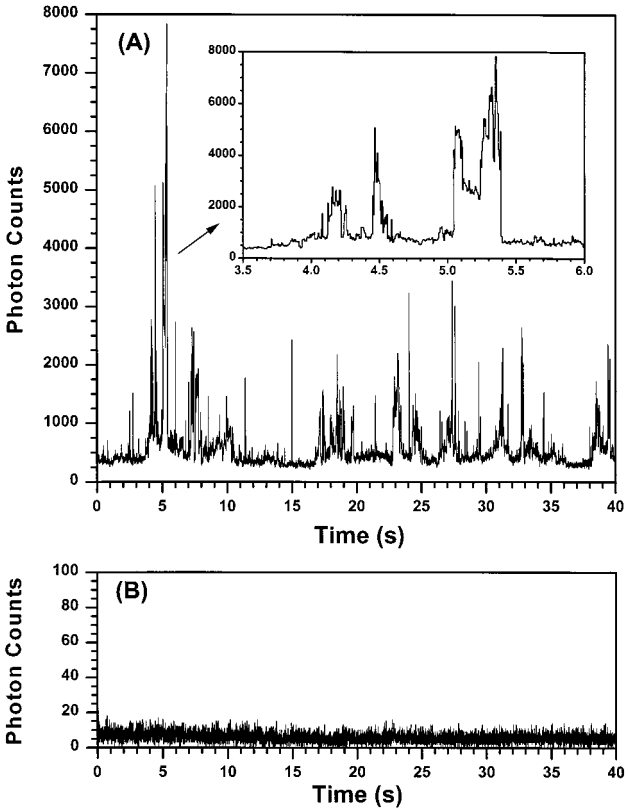

Figure 7. Time-resolved SERS signals of a resonant molecule (crystal violet) adsorbed on a single Au nanoparticle. (A) Total SERS intensity integrated over the spectral region of 500−2000 cm^{-1}. (B) Background (no particle in the laser beam). The inset shows more details of the discontinuous light emission process. Laser wavelength = 647 nm; confocal laser power = 50 μW; and integration time = 5 ms (200 data points per second).

molecules adsorbed on aggregated Au clusters, yielding enhancement factors on the order of $\sim 10^{14}$. The use of near-infrared excitation (830 nm) precludes direct electronic transition, and the observed signals should arise from surface Raman enhancement, with little or no resonance contributions.

Intermittent Light Emission. A further finding is that the SERS-active Au particles emit Raman photons in an intermittent fashion on the millisecond-to-second time scale. This blinking behavior is not apparent in conventional population-based studies due to statistical averaging. Figure 7 shows the time-dependent SERS signals detected from a single Au particle with a photon-counting avalanche photodiode at 200 data points per second. Intermittent SERS is also observed for nonresonant molecules such as bispyridyl ethylene and mercaptopyridine, but with reduced signal intensities (Figure 8). As mentioned earlier, discontinuous photon emission has been reported for a number of single-quantum systems.[7−10] While the true origins of this behavior are still under debate, recent research in several groups indicates that intermittent light emission could arise from long-lived triplet states in single dye molecules,[31] from efficient exciton traps in multichromophore systems,[9,32,33] and from photogenerated quenching centers in CdSe nanocrystals.[10] We have carried out preliminary work to investigate the mechanism of blinking SERS. The results indicate that the blinking frequency (number of peaks per second) is dependent on both

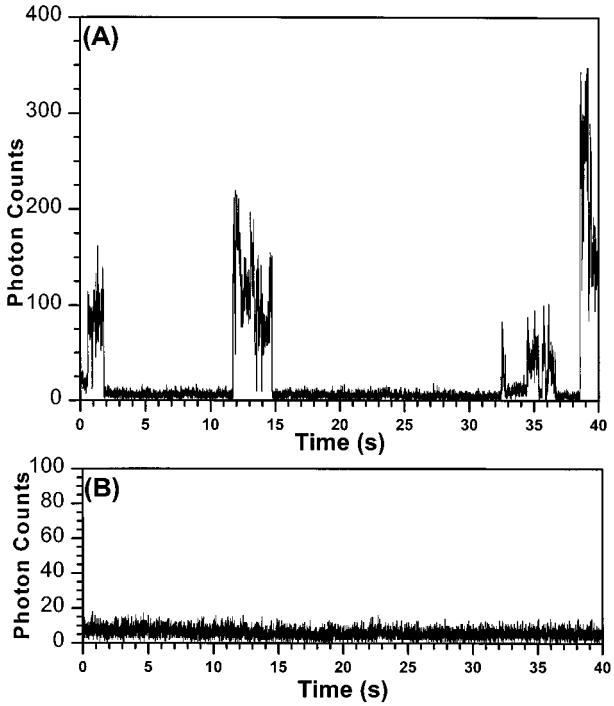

Figure 8. Time-resolved SERS signals of a nonresonant molecule (4-mercaptopyridine) adsorbed on a single Au nanoparticle. (A) Integrated Raman intensity (500−2000 cm^{-1}). (B) Background (no particle in the laser beam). Laser wavelength = 647 nm; confocal laser power = 50 μW; and integration time = 5 ms.

the laser intensity and the sample temperature. Apparently, intermittent SERS can be induced by both thermal activation and optical excitation. Similarly, recent research indicates that intermittent light emission in single CdSe quantum dots contains both thermal and photochemical contributions.[34]

Regardless of its thermal or photoinduced nature, we believe that blinking SERS has only three general mechanisms: (a) changes in the optical properties of the metal nanoparticle, (b) changes in the electronic properties of the adsorbed molecule, and (c) changes in the interaction between the particle and the molecule. If the first mechanism plays a dominant role, it will be primarily an electromagnetic effect caused by fluctuations in the surface plasmon resonance frequencies.[26−28] If the second or the third mechanism is dominant, the blinking signals would come from a single molecule or a single molecular aggregate. The rationale is that multiple molecules adsorbed at different surface sites are unlikely to move or undergo structural changes in a synchronized fashion. As such, they are unlikely to lead to abrupt on/off signal fluctuations (Figures 7 and 8).

Possible single-molecule mechanisms include: (i) photoinduced ionization of an adsorbed molecule (similar to single fluorescent dyes[7−9] and single CdSe quantum dots[10]), (ii) reversible activation and quenching of chemical enhancement at an active site, and (iii) slow diffusion (or desorption) of a single molecule between optically active and inactive sites on the particle surface. The activation energies of surface diffusion and site-to-site hopping are on the order of 5 kcal mol^{-1}, which is well within the reach of low-energy thermal processes. Because the number of active sites on a single particle is very small,[29] surface diffusion will lead to large signal fluctuations. Once a molecule moves out of an active site, it will take a long time for it to find another active site or return to the same site.

(31) Ha, T.; Enderle, Th.; Chemla, D. S.; Selvin, P. R.; Weiss, S. *Chem. Phys. Lett.* **1997**, *271*, 1−5.
(32) Bopp, M. A.; Jia, Y.; Li, L.; Cogdell, R. J.; Hochstrasser, R. M. *Proc. Natl. Acad. Sci. U.S.A.* **1997**, *94*, 10630−10635.
(33) Ying, L.; Xie, X. S. *J. Phys. Chem. B* **1998**, *102*, 10399−10409.
(34) (a) Banin, U.; Bruchez, M.; Alivisatos, A. P.; Ha, T.; Weiss, S.; Chemla, D. S. *J. Chem. Phys.* **1999**, *110*, 1195−1201. (b) Empedocles, S. A., Bawendi, M. G. *J. Phys. Chem. B* **1999**, *103*, 1826−1830.

Our preliminary data indicate that fluctuating SERS signals often occur in clusters, separated by long dark periods (seconds to minutes, see Figure 8). A similar clustering effect has also been observed for single dye molecules that diffuse across a focused laser beam in solution.[24] Thus, the long dark periods are consistent with thermally activated surface diffusion.

A key remaining problem is the structure and properties of active sites on the particle surface. There is considerable evidence in the literature indicating that surface active sites play an important role in SERS.[35] These sites are believed to be adatoms, atomic clusters, sharp steps, or edges. They are responsible for chemical enhancement via resonant charge-transfer and resonance Raman-like enhancement.[36] In other words, strong electronic coupling between an adsorbed molecule and an active site generates new metal-to-ligand or ligand-to-metal charge-transfer states that can be broadly excited at visible wavelengths. Previous work by Hildebrandt and Stockburger[29] suggests that the SERS-active sites are high-affinity binding sites (65 kJ mol^{-1}) associated with adsorbed anions such as Cl^- or Br^-. The number of active sites per colloidal Ag particle is about 3.3 on average, perhaps because there are few sharp points or defects on a faceted Ag nanocrystal.

In conclusion, we have made two fundamental observations on the size-tunable optical properties of small metal particles. A new class of Au colloidal nanopaticles in the size range of 60−70 nm has been identified and characterized that is highly efficient for surface optical enhancement. When coupled with resonance Raman enhancement, these optically "hot" particles allow the detection and identification of single crystal violet molecules. We have also demonstrated that surface enhancement on Au nanoparticles occurs intermittently on the millisecond-to-second time scale. This light emission behavior is strongly dependent on both sample temperature and excitation intensity. A possible mechanism involves photoinduced ionization and thermally activated diffusion of single molecules on the particle surface. It should be pointed out, however, that a complete understanding of the SERS effect is still not available.[37] A major obstacle is that the SERS system (i.e., molecules adsorbed on the surface of small metal particles) is highly complex and heterogeneous. As such, the SERS effect might be best studied and understood at the level of single molecules and single nanoparticles.

Acknowledgment. This work was supported in part by the Department of Energy (FG02-98ER 24873), the National Institutes of Health (R01 GM58173), and the Petroleum Research Fund (32231-AC). S.R.E. acknowledges the Proctor and Gamble Company for a graduate fellowship award, and S.N. acknowledges the Whitaker Foundation for a Biomedical Engineering Award and the Beckman Foundation for a Beckman Young Investigator Award.

JA992058N

(35) Otto, A.; Mrozek, I.; Grabhorn, H.; Akemann, W. *J. Phys. Condens. Mat.* **1992**, *4*, 1143−1212.

(36) Lombardi, J. R.; Birke, R. L.; Tu, T.; Xu, J. *J. Chem. Phys*. **1986**, *84*, 4174. (b) Kambhampati, P.; Child, C. M.; Campion, A. *J. Chem. Soc., Faraday Trans*. **1996**, *92 (23)*, 4775.

(37) Campion, A.; Kambhampati, P. *Chem. Soc. Rev.* **1998**, *27*, 241−250.